Lidar-based closed-loop wake redirection in high-fidelity simulation

Raach, Steffen; Boersma, Sjoerd; Doekemeijer, Bart; Van Wingerden, Jan Willem; Cheng, Po Wen

DOI
10.1088/1742-6596/1037/3/032016

Publication date
2018

Document Version
Final published version

Published in
Journal of Physics: Conference Series

Lidar-based closed-loop wake redirection in high-fidelity simulation

IOP Conf. Series: Journal of Physics: Conf. Series **1037** (2018) 032016 doi:10.1088/1742-6596/1037/3/032016

Lidar-based closed-loop wake redirection in high-fidelity simulation

Steffen Raach[1], Sjoerd Boersma[2], Bart Doekemeijer[2], Jan-Willem van Wingerden[2], Po Wen Cheng[1]

[1]Stuttgart Wind Energy (SWE), University of Stuttgart, Allmandring 5B, 70569 Stuttgart, Germany

[2]Delft University of Technology, Delft Center for Systems and Control, Mekelweg 2, 2628 CD, Delft, The Netherlands

E-mail: raach@ifb.uni-stuttgart.de

Abstract. This work presents the next step in realizing lidar-based closed-loop wake redirection control. Lidar-based closed-loop wake redirection aims at repositioning the wake at a desired position by yawing the wind turbine. The actual wake deflection is derived from lidar measurements and used in a closed-loop control scheme. Compared to an open-loop setting in which temporal changes are not taken into account, lidar-based closed-loop wake redirection can react on temporal disturbances. This yields a more robust control solution due to the employed closed-loop control framework. In this work, for the first time, the concept is implemented in an LES environment namely the PArallelized Large-eddy simulation Model (PALM) code. In PALM lidar measurements are simulated using a lidar model which are processed to estimate the wake position. A controller is synthesized by the usage of a the reduced order wind farm model WindFarmSimulator (WFSim). High-fidelity simulation results illustrate the controller's ability to adapt to a temporal changing crosswind disturbance in a turbulent simulation scenario. Consequently, it increases the power output of the two-turbine scenario compared to the open-loop approach.

1. Introduction

The European Union aims to reach a renewable energy share of 35% by 2020, see [1]. Wind energy is presently seen to be one of the key technologies to meet the future renewable energy goals. The challenges in wind energy research have changed from pioneering the technology to making it financially competitive and mature. Over the years, the size of wind turbines have enormously increased and huge wind farms have been built in which the turbines are clustered. Nowadays, wind farms even reach total energy production capacities 169 GW comparable to conventional power plants (coal: 150 GW, gas: 190 GW), see [2]. With this development, the flow interaction between wind turbines becomes more and more important, since upwind turbines detract the energy yield of downwind turbines.

In the last years, new operational concepts have been developed that have moved from treating the wind turbines individually to considering the wind farm in total. The concepts might lead to suboptimal operation on a turbine level, however, they aim at achieving a global benefit for the wind farm. There are mainly two control objectives that are valid for turbine as well as for wind farm control: maximizing the power output and minimizing the structural loads. In

wind farm operation, the wind turbines interact through their wakes, which are caused by the energy extraction of the turbines. In a wake, the mean wind speed is reduced with respect to the ambient wind speed and the turbulence intensity is increased because of the interaction between the blades and the incoming flow. Two actuation concepts have been studied that aim at mitigating the influences of wakes on other wind turbines: axial induction control and wake redirection control. An elaborate overview of the state-of-the-art in wind farm modeling and control is presented in [3]. This work is in the field of wake redirection control. More precisely, it continues investigations of the lidar-based closed-loop control framework proposed in [4].

Recent studies suggest that wake redirection control has a great potential for improving the performance of a wind farm [5, 6] and is currently under investigation in practice [7, 8]. In general, previously presented methods are based on steady-state models and work with a open-loop control paradigm, resulting in less robust control solutions compared to a closed-loop version. One advanced example of closed-loop wake redirection control can be found in [9] in which time-varying yaw settings are found employing a predictive controller and applied in LES yielding wind farm power increases. In the closed-loop control framework, measurement are taken from the system and used to evaluate new control signals making this paradigm more robust against changes in the environment. Atmospheric changes in the wind farm that occur during relatively short periods are not taken into account in open-loop methods. One example of such an atmospheric change is an alternation in wind direction. In this work, for the first time, the closed-loop wake redirection control strategy [10] is applied in PArallelized Large-eddy simulation Model (PALM) [11]. The in this work applied dynamical closed-loop control strategy makes it possible to take also atmospheric changes into account that occur during a smaller time interval since a continuous feedback is given by the lidar measurements. Therefore, the controller can react much faster to changed conditions than an open-loop approach which is applied based on highly averaged properties.

The paper is structured as follows: First, in section 2, the general concept is summarized and the main objectives are explained. The estimation of the wake position is described in section 3. Then, the controller design is described in section 5 and in section 6, the LES simulation model PALM is summarized. Afterwards, the simulation results are presented in section 7. Finally, conclusions and an outlook on future work are given.

2. Methodology and objectives

Lidar-based closed-loop wake redirection is realized with a local controller on the turbine level that enables the wind farm operator to set desired wake position offsets. This is in contrary to current wake redirection methods in which yaw angels are set. The objective of the concept is to enable the benefits of wake redirection and furthermore use the benefits of closed-loop control to mitigate the disadvantages of open-loop control. The main disadvantages of the latter are the reliability on the model that is used to compute the open-loop yaw angles. Furthermore, the missing knowledge about the real wake position due to a lack of flow measurements in the wake can result in non optimal control. Consequently, the open-loop concept can not react on disturbances like *e.g.* a temporal crosswind or changed atmospheric conditions. Lidar-based closed-loop wake redirection seems to provide a framework that can possibly mitigates those disadvantages. The concept is described in the following.

2.1. Estimation and control task

The basic idea of lidar-based closed-loop wake redirection is to measure the flow behind a wind turbine with a lidar system, estimate the position of the wake, and use the position information in a controller that steers the wake to the desired position. Figure 1 shows the general overview on the concept with the different parts, the estimation and the control task.

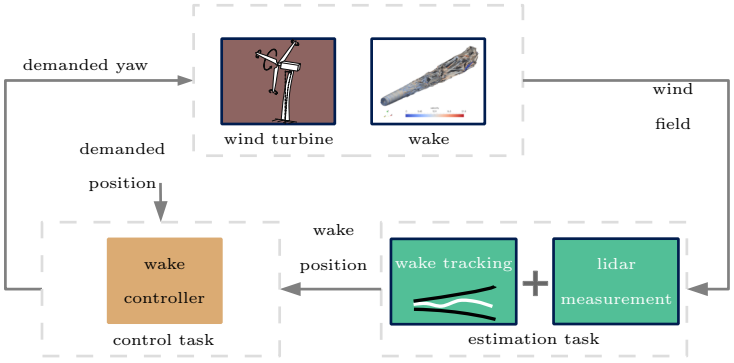

Figure 1. The general concept of lidar-based closed-loop wake redirection.

The estimation task deals with the processing of the lidar measurements and providing an estimate of the actual wake position. Therefore, the measurement data is treated to obtain the estimation at a specified downstream distance, where the lidar is measuring within the flow.

The control task deals with everything related to the wake redirection controller. Generally, it includes the controller design and the implementation of the controller that uses the wake position estimation to steer the wake to a desired position.

2.2. Objectives

The main objective of this work is to demonstrate lidar-based closed-loop wake redirection in an LES code. Further objectives are to demonstrate the benefits of employing the closed-loop dynamical control framework in wake redirection control and to highlight necessary steps in realizing lidar-based closed-loop wake redirection. In detail, the ability to compensate local disturbances on a crosswind is studied.

3. Estimation task

3.1. Lidar model

A lidar model is used, which describes the relation between the flow field and the lidar measurement data. In the lidar model, the components of the flow field are mapped to the line-of-sight measurement of the lidar. A lidar system has two limitations in its measurement principle: 1) the lidar measures only a projection of the flow components onto the laser beam vector, 2) the lidar's volume averaging. For simplicity, the second limitation is neglected in this work and a point measurement is assumed. The limitation would result in a spatial filtering which would simplify the position estimation. The measurement equation for a point measurement is then

$$v_{\text{los}}(x_i, y_i, z_i) = \frac{\left(x_i u_i + y_i v_i + z_i w_i\right)}{\sqrt{x_i^2 + y_i^2 + z_i^2}}, \tag{1}$$

measuring the line-of-sight at the point $[x_i\ y_i\ z_i]$ and the flow vector $[u_i\ v_i\ w_i]$ in that point, see [12]. The lidar obtains line-of-sight wind speed measures simultaneously with a sample time of 2 s at each y- position at hub-height in 3 D (with D the rotor diameter) downwind of the turbine by measuring the flow field. From experiences, 3 D seems to be a sufficient trade-off between time delay and measurability of the wake position and its deflection. Additionally, redirecting the wake at three implies also that the wake is deflected further downstream. Generally, it is more difficult to estimate the wake position from measurements further downstream due to *e.g.* the wake mixing. By measuring only at hub-height some wake effects can not be captured, however it seemed to be sufficient for this demonstration.

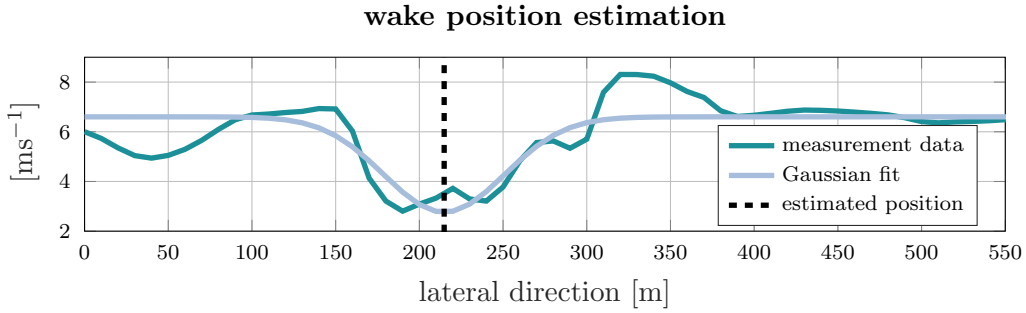

Figure 2. An example of how a Gaussian fit (2) is fitted to measurement data, from which the wake center position can be derived. In this example, $c^{\text{opt}} = \begin{bmatrix} 6.6 & 3.8 & 214.8 & 2592 \end{bmatrix}$, and thus the wake center is estimated to be at $y = 214.8\,\text{m}$ (dashed black line).

3.2. Wake position estimation

An important component of this control framework is the estimation of the wake center position. For this purpose, the processed lidar measurements are leveraged in combination with an assumption on the wake shape. The assumption made here is that the downstream wake deficit follows a Gaussian distribution along the lateral downstream positions at hub height. For the far-wake region, this assumption is in agreement with theoretical and experimental findings [13].

When the wake deficit is modeled to follow a Gaussian curve, the wind speed along the lateral direction (y-direction) at some longitudinal downstream position and turbine hub height can be approximated as:

$$U_{\text{gauss}}(y, c) = c_0 - c_1 e^{\frac{-(y-c_2)^2}{c_3}}. \tag{2}$$

In this equation, c_0 is the freestream velocity, c_1 is the wind speed deficit at the center of the wake, c_2 is the lateral location of the wake center, and c_3 defines the spread (width) of the wake. The wake center is approximated by fitting (2) to the measurements, as

$$c^{\text{opt}} = \arg\min_{c} \left[U_{\text{gauss}}(y_{\text{meas}}, c) - v_{los}(3\,\text{D}, y_{\text{meas}}, z_{\text{HH}})\right]^2, \tag{3}$$

with y_{meas} the y- grid points and the hub-height z_{HH}. Thus, the wake center estimate follows to be c_2^{opt}. (3) is solved using a nonlinear least squares approach. Additionally, the wind speed at the wake center is approximated to be $c_0^{\text{opt}} - c_1^{\text{opt}}$, and the standard deviation of the wake is $\frac{1}{\sqrt{2}}\sqrt{c_3^{\text{opt}}}$. An example is given in figure 2.

Furthermore, note that this methodology can be extended to include multiple wakes by adding a summation sign before c_1 in (2), and introducing a unique set of variables c_1, c_2, and c_3 for each wake.

4. Controller design model

The $\mathcal{H}_\infty$ controller design synthesis of [4] is repeated here to obtain a closed-loop controller. To obtain a controller a linear controller design model is needed. It is chosen according to the procedure described in [4] and is parametrized with simulations performed with the medium-fidelity CFD model WFSim, described in [14]. In the following, first, the methodology is described, then the WFSim model is briefly reviewed and the parametrization is performed to obtain the controller design model.

4.1. Methodology

For the controller synthesis a linear controller design model is needed that gives the dynamic input-output behavior of the system. In this case, the input is the yaw angle and the output the wake position 3 D downstream of the wind turbine, with D the rotor diameter. The general idea is to perform step simulations and use the recorded input and output data to obtain linear models. The methodology has been already used in [10, 15]. To reduce the computational effort LES simulations implicate the step simulations are performed with the medium-fidelity CFD simulation model WFSim. Step simulations at the desired mean wind speed and several yaw setpoints are performed and used in the identification procedure.

In summary, the controller design models are derived with WFSim, the controller is designed and tested in WFSim, and finally implemented in the LES code.

4.2. The medium-fidelity CFD model WFSim

The employed WFSim model is like a two-dimensional model solving for the following equations:

$$\frac{\partial \boldsymbol{u}}{\partial t} + (\boldsymbol{u} \cdot \nabla_H)\boldsymbol{u} + \nabla_H \cdot \boldsymbol{\tau}_H + \nabla_H p - \boldsymbol{f} = 0, \tag{4}$$

$$\nabla_H \cdot \boldsymbol{u} = -\frac{\partial v}{\partial y}. \tag{5}$$

with $\boldsymbol{u} = \begin{pmatrix} u & v \end{pmatrix}^T$ the flow velocity in the x- and y-direction, respectively and p the scaled pressure, see [14] for a detailed derivation of the model. Furthermore, $\nabla_H = (\partial/\partial x, \partial/\partial y)^T$, $\boldsymbol{\tau}_H$ a two-dimensional tensor containing turbulence model. The turbines are modeled based on the actuator disk model (ADM) so that the forcing term $\boldsymbol{f}$ can be defined as:

$$\boldsymbol{f} = \sum_{n=1}^{\aleph} \frac{c_f}{2} C'_{T_n} [U_n \cos(\gamma_n)]^2 \begin{pmatrix} \cos\gamma_n + \varphi \\ \sin\gamma_n + \varphi \end{pmatrix} \mathrm{H}\left[\frac{D}{2} - ||\boldsymbol{s} - \boldsymbol{t}_n||_2\right] \delta\left[(\boldsymbol{s} - \boldsymbol{t}_n) \cdot \boldsymbol{e}_{\perp,n}\right], \tag{6}$$

with $\boldsymbol{s} = (x, y)^T$, H[·] the Heaviside function, $\delta[\cdot]$ the Dirac delta function, $\boldsymbol{e}_{\perp,n}$ the unit vector perpendicular to the n^{th} rotor disk with position $\boldsymbol{t}_n$ and rotor diameter D, U_n the rotor disk flow velocity and φ the averaged wind direction through the farm. Furthermore we have C'_{T_n} the disk-based thrust coefficient, see [14] for more details. In the WFSim model, C'_{T_n} and yaw angle γ_n are considered as the control variables. Furthermore, the scalar c_f in (6) can be regarded as a tuning variable and will in this work be set equal for all turbines in the farm. For the definition of the turbulence model and a more elaborate discussion on the model, we refer to [14]. However, we emphasize that the WFSim model given in (4) and (5) is not a classical two-dimensional model due to the difference in formulation of the continuity equation. In contrast to a standard two-dimensional model, this allows for flow relaxation in the third direction when *e.g.* encountering slow down by a wind turbine. It has been shown in [14] that the WFSim model is capable of estimating wind velocities at hub-height and power data from LES based wind farm models in therein presented cases.

4.3. Model parametrization

For the model parametrization experiments are performed in WFSim by applying input steps to the yaw angle and measure the output that is the wake position at 3 D. These time series are then used to estimate linear dynamic models. Accordingly, step simulations have been performed with homogeneous inflow conditions and a constant wind speed of $U_\infty = 8\,\mathrm{ms}^{-1}$. A 5 deg step on the yaw is applied and the wake position is estimated in 3 D. Figure 3 shows the result of four step experiments. A gray box identification is performed in which the a predefined model structure is parametrized. For the model, four poles and one zero are chosen. A zero is needed because

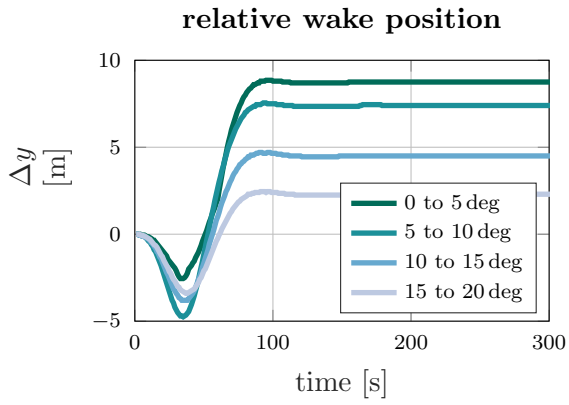

Figure 3. A comparison of different step responses at $8\,\mathrm{ms}^{-1}$. The wake center is estimated 3 D downstream of the wind turbine. For a better comparison the wake position, relative to its initial value is shown.

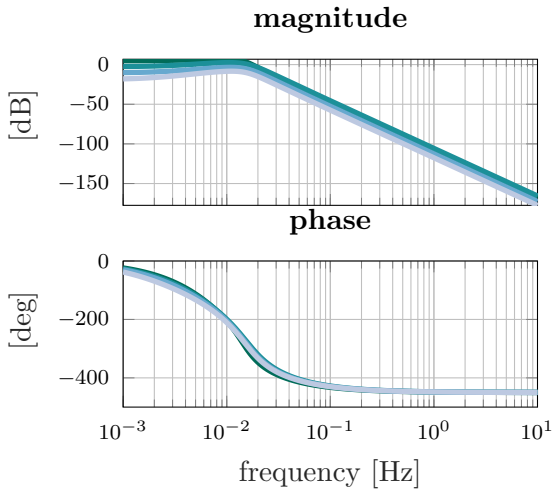

Figure 4. Bode analysis of the parametrized models derived from the step responses of figure 3 (identical color order).

of the inverse response reaction, see figure 3. The cause of the inverse response in the wake position is not yet clear, however it has also been observed in high-fidelity simulations. Four poles gave a very good root-mean-squared error between model output and performed open-loop experiments. In general, more poles and zeros result in an increased number of model states and thus also in an increased number of controller states. Therefore, a minimal representation is sought. This yields the following general model structure

$$G_i(s) = k_i \frac{l_1 s + 1}{(p_1 s + 1)(p_2 s + 1)(p_3 s + 1)(p_4 s + 1)}, \tag{7}$$

with k_i the static gain, $-\frac{1}{l_1}$ the zero, and $-\frac{1}{p_i}$ the poles. A parametrization is performed for all steps which yields the models whose frequency responses are shown in figure 4.

5. Controller design

A $\mathcal{H}_\infty$ controller is designed as described in [10]. The controller design is performed by forming a generalized plant P which consists of the controller design model G, the controller K and weights on the performance outputs z_1, z_2, and z_3. Figure 5 describes the general structure of the generalized plant. The controller design model $G = G_1$ is taken from the identified models because it covers the initial operation range of the controller. The performance outputs give the sensitivity $\mathcal{S}$, the complementary sensitivity $\mathcal{T}$, and the controller sensitivity $\mathcal{U}$, respectively, weighted with the performance weights $W_\mathcal{S}(s)$, $W_\mathcal{T}(s)$, and $W_\mathcal{U}(s)$. The performance weights are used to shape the controller which is found by minimizing the mixed sensitivity problem with respect to $K(s)$

$$\begin{aligned} &\min_K \ \Theta \\ &\text{s.t.} \ \left\| \begin{matrix} W_\mathcal{S}\mathcal{S} \\ W_\mathcal{T}\mathcal{T} \\ W_\mathcal{U}\mathcal{U} \end{matrix} \right\|_\infty \leq \Theta, \end{aligned} \tag{8}$$

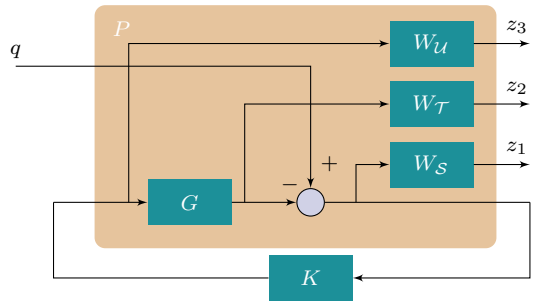

Figure 5. The generalized plant P that consists of the model G, the controller K, the input q, and weights $W_{\mathcal{S}}$, $W_{\mathcal{T}}$, and $W_{\mathcal{U}}$ on the performance outputs z_i.

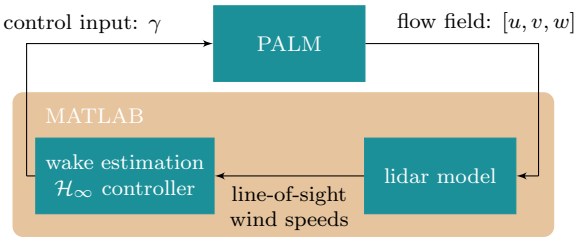

Figure 6. Practical implementation with measurements and control signal utilized in this work.

with

$$\mathcal{S} = \frac{1}{1+GK} \qquad \mathcal{T} = \frac{GK}{1+GK} \qquad \mathcal{U} = \frac{K}{1+GK}. \tag{9}$$

The weights are chosen as described in [10] to mitigate disturbances below the controller bandwidth and to damp control actions at higher frequencies. The latter results in a wake redirection controller that does not react on all oscillations in the wake position. The black plots in figure 7 show the design margins for the controller which result from the weights. The analyses of the sensitivity $\mathcal{S}$ and the controller sensitivity $\mathcal{U}$ are shown and they satisfy the bounds. Figure 8 shows the derived controller.

6. Simulation model

The simulation model employed in this work is The Parallelized Large-Eddy Simulation Model (PALM) [11]. The model is based on the filtered, incompressible Navier-Stokes equations and can represent turbines using the rotating actuator disk model (ADM-R) [16]. The PALM model solves, i.a., for the flow velocities in the x- y- and z-direction (u, v, w, respectively) on a staggered grid. A Matlab/PALM interface has been developed making it possible to import measurements from PALM to Matlab and write control variables from Matlab to PALM at each sample period. The turbine control signals in PALM are the collective pitch angle β, generator torque τ_g and yaw angle γ. In this work, the former two are regulated using a baseline turbine controller [17]. The control signal γ is commanded by the $\mathcal{H}_\infty$ controller. The employed interface and utilized signals are illustrated in figure 6. Simulations are initialized as follows: a fully developed flow field is generated in the precursor with free-stream wind velocities $U_\infty = 8\,\mathrm{ms}^{-1}$, $W_\infty = 0$, and $V_\infty = \tilde{v}(t)$ and a TI_∞ of approximately 5% at hub-height in front of the wind farm. The function $\tilde{v}(t)$ is a time varying function that describes the crosswind perturbation for time step $k+1$

$$\tilde{v}_{k+1} = \begin{cases} \tilde{v}_k + 0.01\tilde{v}_k, & \text{if } k > 550 \text{ and } k < 600, \\ \tilde{v}_k + 0.01\tilde{v}_k, & \text{if } k > 800 \text{ and } k < 850, \\ \tilde{v}_{\mathrm{const}}, & \text{otherwise.} \end{cases} \tag{10}$$

Then, for the specific topology considered in this work, the flow is propagated 900 s in advance with constant control settings so that the wakes are fully developed. Here, non-cyclic boundary conditions and time-dependent turbulent inflow data by using a turbulence recycling method [11] are imposed. The flow field obtained after these 900 s is utilized as initial flow field for the simulation results presented in this work.

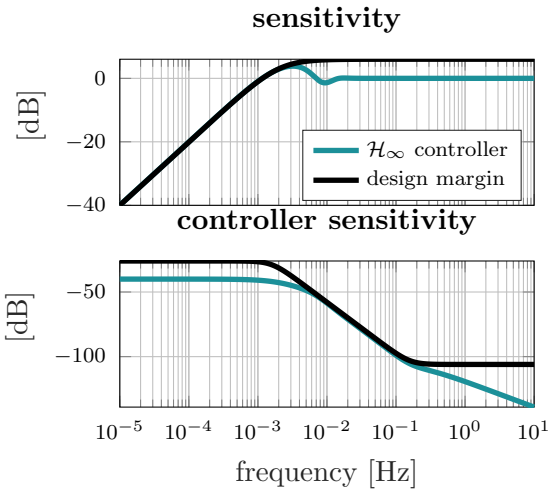

Figure 7. The performance evaluation of the designed controller: The sensitivity $\mathcal{S}$ and the controller sensitivity $\mathcal{U}$. The design margins calculated from the performance weights are shown in black.

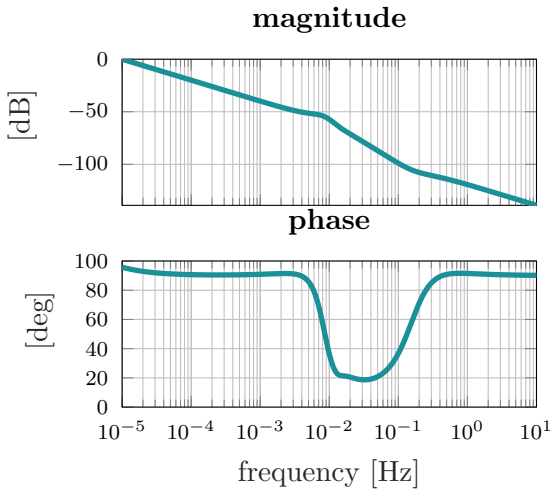

Figure 8. The bode analysis of the designed $\mathcal{H}_\infty$ controller.

Table 1. Summary of the 2-turbine simulation set-up.

Simulation domain	$L_x \times L_y \times L_z$	$10.2 \times 2.5 \times 1.3$ [km^3]
Rotor diameter and hub-height	D, z_h	126, 90 [m]
Grid size	$\Delta x \times \Delta y \times \Delta z$	$10 \times 10 \times 10$ [m^3]
Turbine spacing		$6D$ [m]
Free-stream conditions	$U_\infty, V_\infty, W_\infty$	$8, \tilde{v}(t), 0$ [ms^{-1}]
Turbulence intensity	TI_∞	5%
Simulation time	N	1000 [s]
Sample period	Δt	1 [s]
Position of turbine 1	Cx_1, Cy_1	300, 220 [m]
Position of turbine 2	Cx_2, Cy_2	1020, 340 [m]

7. Simulation results

In a test scenario, the proposed dynamical yaw controller is applied to a NREL 5MW turbine [17]. A summary of the simulation setup is presented in Table 1. At $t = 100\,\mathrm{s}$, the controller is switched on and a crosswind disturbance is added. The disturbance yields a shift of the wake position in direction of the crosswind, see figure 9. This is due to the controller that counteracts the crosswind and adapts to the disturbance. The wake position is in the closed-loop case steered closer to the reference signal, but stays oscillating because of *e.g.* wake meandering. Time averaging the measurement results in less oscillatory behavior though will also reduce the bandwidth of the closed-loop controlled system. Applying the closed-loop controller yields an increased total power output of 2.9% over the simulation horizon with respect to the open-loop case. This is due to the fact that the second turbine is influenced less by the wake of the first turbine under the introduced cross-wind perturbation, see figure 10 and figure 11.

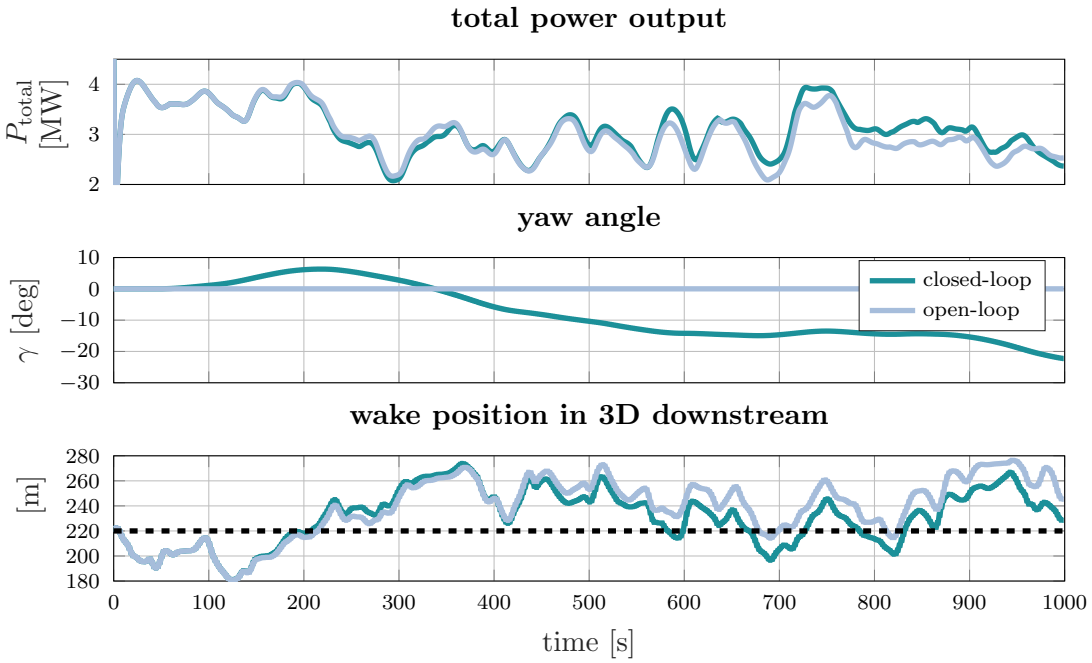

Figure 9. A comparison of two simulations, an open-loop and a closed-loop simulation, where crosswind is disturbing the wake positioning. The sample time of the controller is $5s$. The desired wake position is indicated in black.

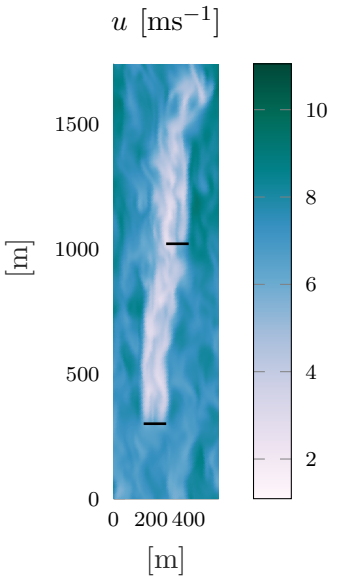

Figure 10. Open-loop flow snapshot at $t = 800\,\text{s}$.

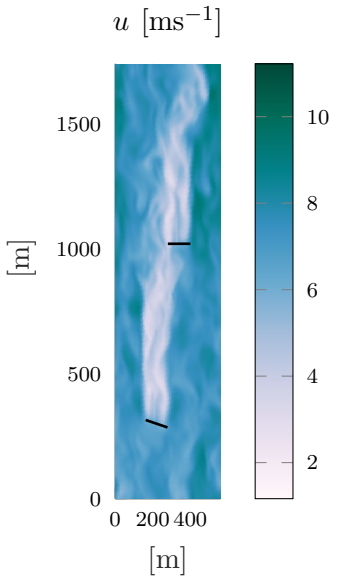

Figure 11. Closed-loop flow snapshot at $t = 800\,\text{s}$.

8. Conclusions and future work

In this work an implementation of lidar-based closed loop wake redirection in the LES simulation model PALM was presented. The controller was synthesized by using a medium-fidelity CFD simulation model in which an input-output model parametrization was performed. In a $\mathcal{H}_\infty$ controller synthesis methodology, a controller for closed-loop wake redirection was derived. A case study with a time-varying signal, cross-wind is used to illustrate the benefit of employing a closed-loop yaw controller. In the open-loop case, due to the cross-wind perturbation, the wake of the upwind turbine will overlap the downwind turbine's rotor reducing its power production. However, in the closed-loop case, the dynamical feedback yaw controller redirects the wake such that less wake overlap occurs and the overall power production is increased over the simulation horizon. In other words, the simulation case presented here illustrates the possible advantage of the closed-loop approach by being able to react on disturbances. In future work, a combination of the open-loop and closed-loop approach will be derived. It will compute the open-loop yaw angles and will use them in a feedforward controller augmented with a closed-loop controller as the one presented in this work. Furthermore, the lidar measurements will be extended to a more realistic model and measurement setup.

Acknowledgements

The authors would like to thank Sonja Krüger and Gerald Steinfeld from ForWind (Oldenburg) and Will van Geest (TU-Delft) for their valuable input regarding the PALM simulations.

Furthermore, the CL-Windcon project is acknowledged which has received funding from the European Union's Horizon 2020 research and innovation programme under grant agreement No 727477.

References

[1] WindEurope Business Intelligence 2017 Wind energy in Europe: Outlook to 2020
[2] WindEurope Business Intelligence 2018 Wind in power 2017 - Annual combined onshore and offshore wind energy statistics
[3] Boersma S, Doekemeijer B M, Gebraad P M O, Fleming P A, Annoni J, Scholbrock A K, Frederik J A and van Wingerden J W 2017 A tutorial on control-oriented modelling and control of wind farms *Proceedings of the American Control Conference (ACC)*
[4] Raach S, Schlipf D and Cheng P W 2017 *Wind Energy Science*
[5] Gebraad P M O, Teeuwisse F W, van Wingerden J W, Fleming P A, Ruben S D, Marden J R and Pao L Y 2014 *Wind Energy*
[6] Campagnolo F, Petrović V, Schreiber J, Nanos E M, Croce A and Bottasso C L 2016 *Journal of Physics: Conference Series* **753** 032006
[7] Fleming P, Annoni J, Scholbrock A, Quon E, Dana S, Schreck S, Raach S, Haizmann F and Schlipf D 2017 *Journal of Physics: Conference Series* **854** 012013
[8] Fleming P, Annoni J, Shah J J, Wang L, Ananthan S, Zhang Z, Hutchings K, Wang P, Chen W and Chen L 2017 *Wind Energy Science* **2** 229–239
[9] Munters W and Meyers J 2018 *Energies* **11** 177 ISSN 1996-1073
[10] Raach S, van Wingerden J W, Boersma S, Schlipf D and Cheng P W 2017 Hinf controller design for closed-loop wake redirection *Proceedings of the American Control Conference (ACC)* (Seattle, USA) pp 703–708
[11] Maronga B, Gryschka M, Heinze R, Hoffmann F, Kanani-Sühring F, Keck M, Ketelsen K, Letzel M O, Sühring M and Raach S 2015 *Geoscientific Model Development*
[12] Schlipf D 2016 *Lidar-assisted control concepts for wind turbines* Ph.D. thesis University of Stuttgart
[13] Bastankhah M and Porte-Agél F 2016 *Journal of Fluid Mechanics*
[14] Boersma S, Doekemeijer B M, Vali M, Meyers J and van Wingerden J W 2018 *Wind Energy Science*
[15] Raach S, Boersma S, Wingerden J W, Schlipf D and Cheng P W 2017 *International Federation of Automatic Control*
[16] Dörenkämper M, Witha B, Steinfeld G, Heinemann D and Kühn M 2015 *Journal of Wind Engineering and Industrial Aerodynamics*
[17] Jonkman J M, Butterfield S, Musial W and Scott G 2009 Definition of a 5-MW reference wind turbine for offshore system development Tech. rep. National Renewable Energy Laboratory (NREL)